



Precipitation isoscape of high reliefs: interpolation scheme designed and tested for monthly resolved precipitation oxygen isotope records of an Alpine domain

Z. Kern^{1,2,3}, B. Kohán⁴, and M. Leuenberger^{1,2}

¹Division of Climate and Environmental Physics, Physics Institute, University of Bern, Bern, Switzerland

²Oeschger Centre for Climate Change Research, Bern, Switzerland

³Institute for Geological and Geochemical Research, Research Centre for Astronomy and Earth Sciences, MTA, Budapest, Hungary

⁴Dept. of Environmental and Landscape Geography, Eötvös University, Budapest, Hungary

Correspondence to: M. Leuenberger (leuenberger@climate.unibe.ch)

Received: 24 March 2013 – Published in Atmos. Chem. Phys. Discuss.: 15 April 2013

Revised: 28 December 2013 – Accepted: 14 January 2014 – Published: 18 February 2014

Abstract. Stable oxygen isotope composition of atmospheric precipitation ($\delta^{18}\text{O}_p$) was scrutinized from 39 stations distributed over Switzerland and its border zone. Monthly amount-weighted $\delta^{18}\text{O}_p$ values averaged over the 1995–2000 period showed the expected strong linear altitude dependence (-0.15 to -0.22 ‰ per 100 m) only during the summer season (May–September). Steeper gradients (~ -0.56 to -0.60 ‰ per 100 m) were observed for winter months over a low elevation belt, while hardly any altitudinal difference was seen for high elevation stations. This dichotomous pattern could be explained by the characteristically shallower vertical atmospheric mixing height during winter season and provides empirical evidence for recently simulated effects of stratified atmospheric flow on orographic precipitation isotopic ratios. This helps explain “anomalous” deflected altitudinal water isotope profiles reported from many other high relief regions. Grids and isotope distribution maps of the monthly $\delta^{18}\text{O}_p$ have been calculated over the study region for 1995–1996. The adopted interpolation method took into account both the variable mixing heights and the seasonal difference in the isotopic lapse rate and combined them with residual kriging. The presented data set allows a point estimation of $\delta^{18}\text{O}_p$ with monthly resolution. According to the test calculations executed on subsets, this biannual data set can be extended back to 1992 with maintained fidelity and, with a reduced station subset, even back to 1983 at the expense of faded reliability of the derived $\delta^{18}\text{O}_p$ estimates,

mainly in the eastern part of Switzerland. Before 1983, reliable results can only be expected for the Swiss Plateau since important stations representing eastern and south-western Switzerland were not yet in operation.

1 Introduction

Stable isotopes of past and present precipitation are important natural tracers in the hydrological cycle on global, regional and local scales and are permanently in the focus of environmental isotopic studies. Owing to the growing number of monitoring stations for isotopic composition of atmospheric precipitation worldwide and the great technical advance in geostatistical treatment of geochemical data via geographic information system (GIS)-based spatial modelling tools (Bowen, 2010a), precipitation isotope mapping has revolutionized over the past decade.

Precipitation isoscape (isotopic landscape) is a map of isotopic variation produced by an iteratively applied predictive model to estimate the local isotopic composition of precipitation as a function of observed local and/or extralocal environmental variables across regions of space using gridded environmental data sets (Bowen, 2010a; West et al., 2010). The first isoscape of global precipitation was derived by Bowen and Wilkinson (2002). Later on, Bowen and Revenaugh (2003) proved that geostatistical

approaches undeniably outperform simple interpolation techniques. These advances fertilized numerous studies on regional precipitation isoscapes (Meehan et al., 2004; Liebinger et al., 2006; Lykoudis and Argiriou, 2007; Lykoudis et al., 2010; Vachon et al., 2010; Holko et al., 2012; Welker, 2012; Liotta et al., 2013, Hunjak et al., 2013). Nowadays, the geostatistical approach is a popular technique for the mapping of precipitation water isotope ratios (Bowen, 2010b).

Although these studies have dominantly pictured the long-term mean isotopic landscape of the region, recently and occasionally the average seasonal cycle is also tracked (Vachon et al., 2010; Welker, 2012). Hitherto, only one study made an attempt to generate a monthly resolved gridded data set employing a geostatistical method over the eastern Mediterranean region (Lykoudis et al., 2010). However, the application fields (ecology, hydrology or forensic) that motivated the evolution of precipitation isoscapes would surely benefit more if the temporal differences could be followed as well. This will open up new perspectives in isoscape applications, i.e. dynamic applications. This recognition inspired us to focus in the present study on monthly stable oxygen isotope compositions of atmospheric precipitation (hereafter $\delta^{18}\text{O}_p$). It is worth mentioning that the latest released global precipitation isoscape (Terzer et al., 2013) employed a regionalized approach, using 36 statistically defined climatic spatial domains rather than any fixed general equation providing explicit justification for regional isoscape derivation efforts. A characteristic landscape, where large-scale isotope mapping and isoscape derivation efforts frequently report failure or experience major uncertainties, is one with high reliefs (e.g. Bowen and Revenaugh, 2003; Terzer et al., 2013). This is not surprising at all regarding their complex topography and the dynamical interactions with micro- and mesoscale processes of cloud physics (Rotunno and Houze, 2007), which obviously are linked to isotopic fractionation processes taking place during the aggregation and fall of hydrometeors. However, intriguingly, high reliefs are prime target areas of important applications, i.e. palaeoaltimetry based on authigenic minerals and (palaeo)climatology based on ice core-derived stable water isotope records, where sound knowledge about the detailed spatial features of water isotopes is crucial.

The central assumption of palaeoaltimetry based on $\delta^{18}\text{O}$ measured from authigenic minerals – besides the fact that their oxygen was derived from meteoric water – is the general observation of decreasing $\delta^{18}\text{O}$ values in rainfall as elevation increases (Rowley and Garzione, 2007). However, the methodological background of palaeoaltimetry is under severe criticism recently. Both past climate changes (Ehlers and Poulsen, 2009) and landscape evolution (Galewsky, 2009) have been shown to have an impact on precipitation isotopic signature in the absence of any uplift and thereby significantly alter palaeoaltimetry interpretations.

Under certain glaciological constraints, glacial ice bodies from high reliefs are precious archives of past precipitation (Schwikowski and Eichler, 2010), and isotopic compo-

sition of ice cores is often interpreted as temperature proxy (e.g. Baker et al., 1985; Thompson et al., 1995; Schöner et al., 2002). However, a growing body of evidence illustrates that isotopic composition of ice cores carries more complex atmospheric signal rather than being a simply temperature proxy (Schotterer et al., 1997). A recent study found weak, if any, agreement to proximal sites computing spatial correlation between ice core-derived isotope records of the Alps to regional high resolution climate field data (Mariani et al., 2012). In addition, practically all previous precipitation isoscape mapping products were based upon amalgamated discontinuous long-term data sets, and therefore these mapping efforts had an inherent assumption of temporal constancy in their predictive outcomes (Terzer et al., 2013). However, this assumption is not valid for the European Alps, for instance, because significant decadal trends were detected in the Alpine $\delta^{18}\text{O}_p$ records (e.g. Schotterer et al., 2000).

All these findings illuminate that a better understanding of water isotopes of precipitation over high reliefs is needed.

The Alps host the oldest and densest network monitoring of stable isotopes of atmospheric precipitation compared to any other mountainous area of the world, owing to the good representation of international (GNIP) and national (Switzerland and Austria) networks. Detailed assessments conducted on these data have substantially contributed to our knowledge about isotopic processes acting and interacting at various spatial and temporal scales in the atmosphere, or more generally in geospheres (e.g. Siegenthaler and Oeschger, 1980; Liebinger et al., 2007; Fröhlich et al., 2008).

The relative wealth of long-term and regular monitoring data offer a great opportunity to initiate a kind of time-series approach to $\delta^{18}\text{O}_p$ isoscapes in this region. The motivation for the research was to develop a gridded data set of monthly $\delta^{18}\text{O}_p$ over Switzerland and adjacent areas with high spatial resolution back to the early 1970s. In the present paper only the methodological background will be discussed and interpolations on $\delta^{18}\text{O}_p$ are provided for 1995 and 1996, when the station network was the densest, in order to check whether a reduced number or subset of stations could reproduce the same spatial patterns captured by the full data set. Furthermore, we hope that this exceptional station collection will improve the understanding of stable isotope spatial pattern over a high relief, providing useful information to studies focused on other mountainous regions poorly covered by direct measured data.

2 Material and methods

2.1 Stable oxygen isotope ratios from precipitation

Measurements of oxygen isotope ratios in precipitation started as early as 1965 at Thonon-les-Bains (France) and 1971 at Bern in the Alpine region. However, the network

was very sparse during the first years. Station density significantly improved only from 1973 when more Swiss and Austrian stations became involved into the network.

We gathered 43 monthly resolved $\delta^{18}\text{O}_p$ records from the region. Basic information about these stations is listed in Table S1. This collection was constructed from the following sources mentioned below.

Swiss National Network for Observation of Isotopes in the Water Cycle (NISOT) (Schürch et al., 2003, Schotterer et al., 2010) is represented by 6 + 5 stations. The +5 stations are also included in the Global Network of Isotopes in Precipitation (GNIP) (IAEA, 2010). The GNIP is represented by an additional 5 stations in Germany and one station in France. The Austrian Network of Isotopes in Precipitation (ANIP) (Kralik et al., 2003) is represented by 9 stations in Vorarlberg and Tyrol.

Eight relatively shorter records were available from northern Italy (Longinelli and Selmo, 2003, 2006). And finally, the Division of Climate and Environmental Physics, Physics Institute, University of Bern, ran an extended network with 9 stations until 2010. It is worth emphasizing that this is the first publication of these invaluable multidecadal monitoring records. Only sparse records (e.g. Schotterer et al., 1997) or mean values (Schotterer et al., 2010) were published previously.

Spatial and temporal distribution of the records is presented in Figs. 1 and S1. We note that available station records frequently suffer from data gaps; Bern and Grimsel are the only stations that provide continuous records. Hence, as an accidental benefit, these gaps may be filled with the retrieved information from neighbouring stations based on the proposed interpolation employing advanced geostatistical tools.

Station density was the highest (0.17–0.18 station per 1000 km², $n = 39$) in 1995–1996 (Fig. S1), while the period (> 5 yr) for which amount-weighted isotope values could be calculated using the widest subset was 1995–2000. This population of 39 stations corresponds to almost twice as many as were available for the much more expanded domain of the eastern Mediterranean during the best represented period of the Mediterranean isoscape (Lykoudis et al., 2010).

Two steeper increases can be discerned in the temporal station density curve (Fig. S1). These are linked to significant expansions of the network: (i) the early 1980s when the network of the Division of Climate and Environmental Physics, Physics Institute of the University of Bern, was initiated and the station density exceeded 0.10 station per 1000 km²; and (ii) in the early 1990s when NISOT and the two earliest northern Italian stations were launched and the station density exceeded 0.14 station per 1000 km². The 12 longest-running station records have been (almost) continuously available since 1973, providing a station density of 0.06 station per 1000 km². These key periods were regarded when reduced subsets were designated. These 12 and another 24 longest-running station records would allow extending the

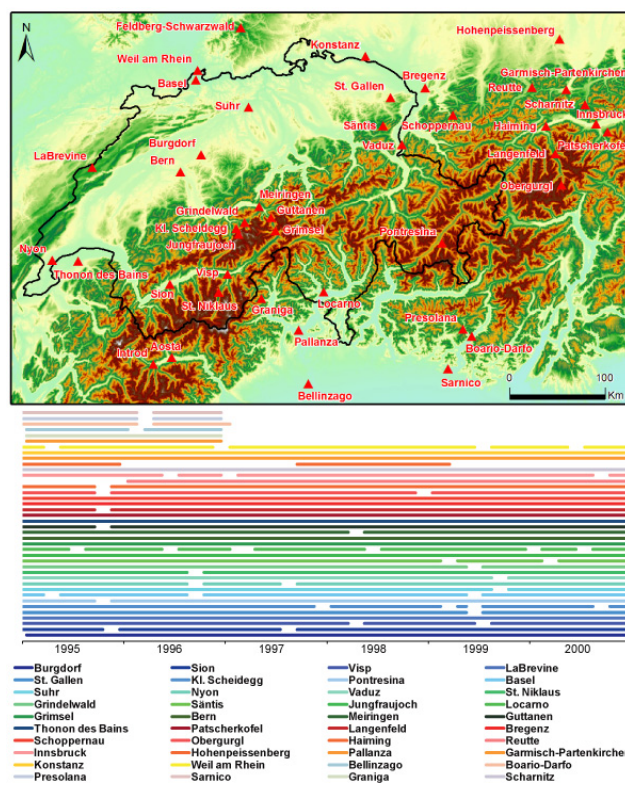


Fig. 1. Spatial distribution of the 43 stations with available records of monthly stable oxygen isotope ratio of precipitation over Switzerland and its border region. Temporal distribution is shown between 1995 and 2000. (Data sources: NISOT (Schürch et al., 2003), ANIP (Kralik et al., 2003), GNIP (IAEA, 2010), N-Italy (Longinelli and Selmo, 2006, 2003) and the network run by the Division of Climate and Environmental Physics, Physics Institute, University of Bern).

mapping back to 1973 and 1984. The entire network offers the early 1990s as the starting date for isoscape generation.

However, the first mandatory step was to test the spatial consistency among the networks. Therefore we compared nearby station records by visual inspection and regression analyses (Fig. S2). The very good agreement among the nearby records ascertained the merging of the networks.

We used the monthly precipitation totals for the Swiss stations (NISOT, KUP and the five IAEA stations from Switzerland) provided by the MeteoSwiss and the precipitation records provided in the corresponding data set (e.g. ANIP, GNIP) for each station to calculate the amount-weighted monthly and annual $\delta^{18}\text{O}_p$ values for the 1995–2000 period. The only exception was Jungfrauoch (JFJ) where MeteoSwiss does not run official precipitation monitoring. Besides snow collection for isotope analysis weights of monthly snow accumulation were records for 228 months between June of 1990 and December of 2010 at JFJ. However, this record seemed to be biased until December 1993 (lower mean, dampened variance) compared to the neighbouring

rain gauge records. The reliable subset (1994–2010) encompassed 117 monthly values and provided the strongest correlation to Grindelwald and Kleine Scheidegg with $R^2 = 0.51$ and 0.46 , respectively (Fig. S3). A complete series of monthly weights has been estimated for JFJ based on a bilinear regression using Grindelwald and Kleine Scheidegg records as predictors. Despite the fact that these derived values are not an accurate measure of the absolute accumulation, any proportional weights are sufficient for the purpose of calculation of amount-weighted mean isotopic parameters.

Precipitation data from MeteoSwiss are quality controlled on a daily basis, partly by manual inspection and also by computer-assisted automated spatio-climatological approach (Scherrer et al., 2011). Earlier evaluation of the Alpine rain-gauge records reported variable quality status from various data providers (Frei and Schär, 1998). From our region of interest, southern Germany and south-east France were found to be thoroughly controlled (range test, spatial consistency) while relatively poorer data quality was found for northern Italy. Different daily reading times (e.g. 07:00 CET in Austria; 07:30 in Switzerland; 09:00 in Italy) (Frei and Schär, 1998) might also introduce further inconsistencies; however, its significance is very likely vanished for monthly totals. Uncertainties with precipitation amount definitely introduce some bias into amount-weighted $\delta^{18}\text{O}$ data.

2.2 Planetary boundary layer

Monthly average maximum daytime planetary boundary layer (PBL) height above the region (data derived from a $1^\circ \times 1^\circ$ grid, von Engel and Teixeira, 2013) was corrected for the corresponding grid-cell reference surface (derived from the hypsometric data of the same $1^\circ \times 1^\circ$ cell). The corresponding subset of the Shuttle Radar Topography Mission (SRTM) database (Farr et al., 2007) was used as reference terrain. Due to the further grid manipulations, the coarse spatial resolution of the original PBL data set was equalized to the 100 m resolution of the SRTM digital elevation model (DEM), applying ordinary kriging interpolation (Cressie, 1993). Graphical illustration of the PBL derivation can be found in the Supplement (Fig. S4).

Seven different methods for determining the PBL height were tested by von Engel and Teixeira (2013). To avoid mistaken detection of near surface inversion as a very low PBL height, all data below 50 m were excluded from the analysis. Overall, the methods associated with the identification of vertical gradients of either relative humidity PBL_{RH} , potential temperature PBL_{Tp} , or virtual temperature PBL_{Tv} appeared to be the most robust. From compared PBL climatologies based on these methods, it was concluded that (i) the two temperature-based methods produce very similar results, and (ii) PBL_{RH} showed large variability over mountainous regions (for instance, over the Alps) for all seasons. Therefore we used PBL_{Tp} in our analysis.

2.3 Interpolation and mapping

Our primary intention was to adopt a method designed for the global isoscape (Bowen and Wilkinson, 2002). Regarding the relatively small spatial domain and the accompanied large orographic complexity, however, the consensus opinion in the Alps is that height effect dominates the Alpine $\delta^{18}\text{O}_p$ (Siegenthaler and Oeschger, 1980; Schürch et al., 2003). Our experience agreed with this opinion as residuals after the removal of the height effect did not show any significant correlation with either latitude or longitude. The south–north contrast was discernible in the residuals, in line with expectations (Sodemann and Zubler, 2010), meaning that the northern Italian sites and Locarno from Ticino tended to define a separate cluster with characteristically less depleted values compared to the rest of the domain. This surely mirrors the combined effect of the characteristically drier air and the closely linked, isotopically distinct, moisture source of these Mediterranean-exposed regions (Frei and Schär, 1998).

Therefore, only the altitude was employed as predictor and any regional difference in vapour source effect or relative humidity was decided to be treated in the residual field by spatial interpolation, similarly to Bowen and Revenaugh (2003) or Lykoudis et al. (2010). We note that this is not an extraordinary simplification. An isotopic contour map of precipitation in Sicily, for instance, having a commensurable extension to our study domain, was also derived using only regional height effect and DEM-derived elevation (Liotta et al., 2013).

Regarding the seasonally variable vertical $\delta^{18}\text{O}_p$ structure (see Sect. 3.1), a 4-step approach was designed for interpolation, taking into consideration the monthly PBL heights. Interpolation was calculated using ordinary kriging. Obtained grids (with 100 m resolution) were exported to .asc format and further grid and raster manipulation were managed in ArcGIS 10 (ESRI INC. 2010) using the Spatial Analyst module.

Step 1 – PBL truncated DEM: to get the PBL truncated DEM surface grid points ($Z_{i,j}$) of the actual month (Z^t , $t = \text{January } 1995, \dots, \text{December } 1996$), a conditional structure was used from the ArcGIS Spatial Analyst Raster Calculator:

$$Z_{i,j}^t = \text{Con}(\text{PBL}_{i,j}^t > \text{DEM}_{i,j}, \text{DEM}_{i,j}, \text{PBL}_{i,j}^t). \quad (1)$$

Step 2 – Monthly initial grids: these were computed from this surface using the regression equations obtained from the below-PBL stations (1995–2000) as follows:

$$\delta^{18}\text{O}_{\text{ini}}^t = S_m \cdot Z_{i,j}^t + b_m \quad (2)$$

where S_m and b_m ($m = \text{January}, \dots, \text{December}$) are the slope and offset of the corresponding monthly regression equation, respectively. The operation was carried out with the ArcGIS Spatial Analyst Raster Calculator tool.

Step 3 – Residual kriging: values from the monthly initial grids were subtracted from the corresponding raw monthly

station data and it was assumed that only the horizontal dependencies are retained in the obtained residuals ($\delta^{18}\text{O}_{\text{res}}$). They were interpolated to the same grid using ordinary kriging (Cressie, 1993).

Step 4 – Final map: corresponding initial and residual grids were summed:

$$\delta^{18}\text{O}_{\text{p}}^f = \delta^{18}\text{O}_{\text{ini}}^f + \delta^{18}\text{O}_{\text{res}}^f. \quad (3)$$

3 Results and discussion

3.1 Seasonal pattern in the oxygen isotopic lapse rate

The expected strong altitude dependence (Siegenthaler and Oeschger, 1980) was evident only for summer months (-0.15 to -0.22 ‰ per 100 m). Steeper gradients (-0.56 to -0.60 ‰ per 100 m) were observed for winter months over a low elevation belt, while hardly any altitudinal difference was seen for high elevation stations. This dichotomy can also be observed, though to a lesser degree, during spring and autumn (Fig. 2).

Similar deviations were observed for summit stations in the Alps even at the dawn of atmospheric isotopic studies (Ambach et al., 1968; Siegenthaler and Oeschger, 1980) and were also reported very recently for other European mountain ranges (Holko et al., 2012), but proper explanation is still missing. Lack of altitude dependence in δD for fresh snow samples collected in the early 1970s was reported above a certain height (~ 3900 m) from the Mt. Blanc region (Moser and Stichler, 1974). As these high elevation samples stood out from the general trend, they were tagged as “high degree of deviation” and were not considered in the evaluation. A later study reported a major discontinuity, called “iso δ -step”, in the variation of $\delta^{18}\text{O}$ (and δD) with altitude in the Saint Elias Mountains (Holdsworth et al., 1991).

As these observations relied on surface snow samples, post depositional changes in the surface snow (Moser and Stichler, 1974) could not be excluded and distinct snow events collected during sampling episodes might also have complicated the interpretation (Holdsworth et al., 1991). Our data set consists exclusively of monthly precipitation samples; therefore, any post-depositional process can definitely be excluded and the found isotopic pattern must be related to atmospheric processes. In addition, owing to the relatively great number of stations collected in the present data set and their relatively dense coverage, throughout the full Alpine elevation range monthly plots allowed to capture the seasonal pattern of this elevational decoupling. Finally, the regular multianual monitoring guarantees that the observed trend distortion of the presented Alpine vertical isotopic profile cannot be explained by an occasional anomaly or a haphazard mixture of distinct precipitation events.

Our working hypothesis was that the lower atmospheric mixing height is mirrored in this pattern, since it is well-known that atmospheric mixing height is low during winter

and significantly higher during summer over Europe (Seidel et al., 2012; von Engel and Teixeira, 2013). PBL is usually situated at or above the Alpine summits (Nyeki et al., 2000; Henne et al., 2004) during summer; hence it does not affect the aestival vertical isotopic pattern.

To test this hypothesis, planetary boundary layer (PBL) levels were approximated (see Sect. 2.2). Afterwards stations were grouped by considering their relative position to the PBL (i.e. above or below PBL). This comparison nicely confirmed our suspicion as visually placed breakpoints of the scatter plots regularly corresponded to the PBL separated station groups (Fig. 2).

3.2 $\delta^{18}\text{O}_{\text{p}}$ profiles and their relation to atmospheric static stability

Precipitation mechanisms over high reliefs vary according to the prevailing flow regime, i.e. whether the flow at low elevations is unblocked and easily rises over the barrier or if it is blocked or retarded in such a way that a relatively stagnant or slow-moving layer of air lies underneath the more rapidly rising air. In both cases, smaller-scale embedded cellular air motions occur and play a role in the enhancement of the growth processes of hydrometeors, but the nature of the smaller-scale cellular motions is different in these two basic flow regimes (Rotunno and Houze, 2007).

A water isotopologue-enabled idealized model suggested significant differences in the potential vertical distribution of orographic precipitation isotopic ratios, depending on the orogenic morphology, the wind speed or the atmospheric static stability (Galewsky, 2009).

To estimate the characteristic seasonal difference in static stability of the Alpine region, squared moist Brunt–Väisälä frequency (N_{m}^2) has been estimated as

$$N_{\text{m}}^2 = \frac{g}{T} \times (\Gamma_0 + \Gamma_{\text{m}}), \quad (4)$$

where g is the gravitational acceleration, T is the sensible temperature, and Γ_0 and Γ_{m} are ambient and moist adiabatic lapse rates, respectively. Durran and Klemp (1982) showed that this simplified formulation produces a reasonably good approximation of the moist Brunt–Väisälä number.

Seasonal difference in static stability has been calculated for the southern and northern side of the Alpine orographic complex separately, regarding the sharp climate contrast between the south and north side of the Alpine ridge. Monthly mean temperatures have been extracted from the ECA&D (European Climate Assessment & Dataset) E-Obs database (Haylock et al., 2008) over a similar domain at the northern (8 – 10° E, 47.25 – 47.5° N) and southern (8 – 10° E, 45.25 – 45.5° N) Alpine foothills and have been averaged for the 1995–2000 period. Summer and winter empirical lapse rates have been derived from a recent compilation based on carefully homogenized absolute temperature records (Chimani et al., 2013), while monthly lapse rate values for the transition

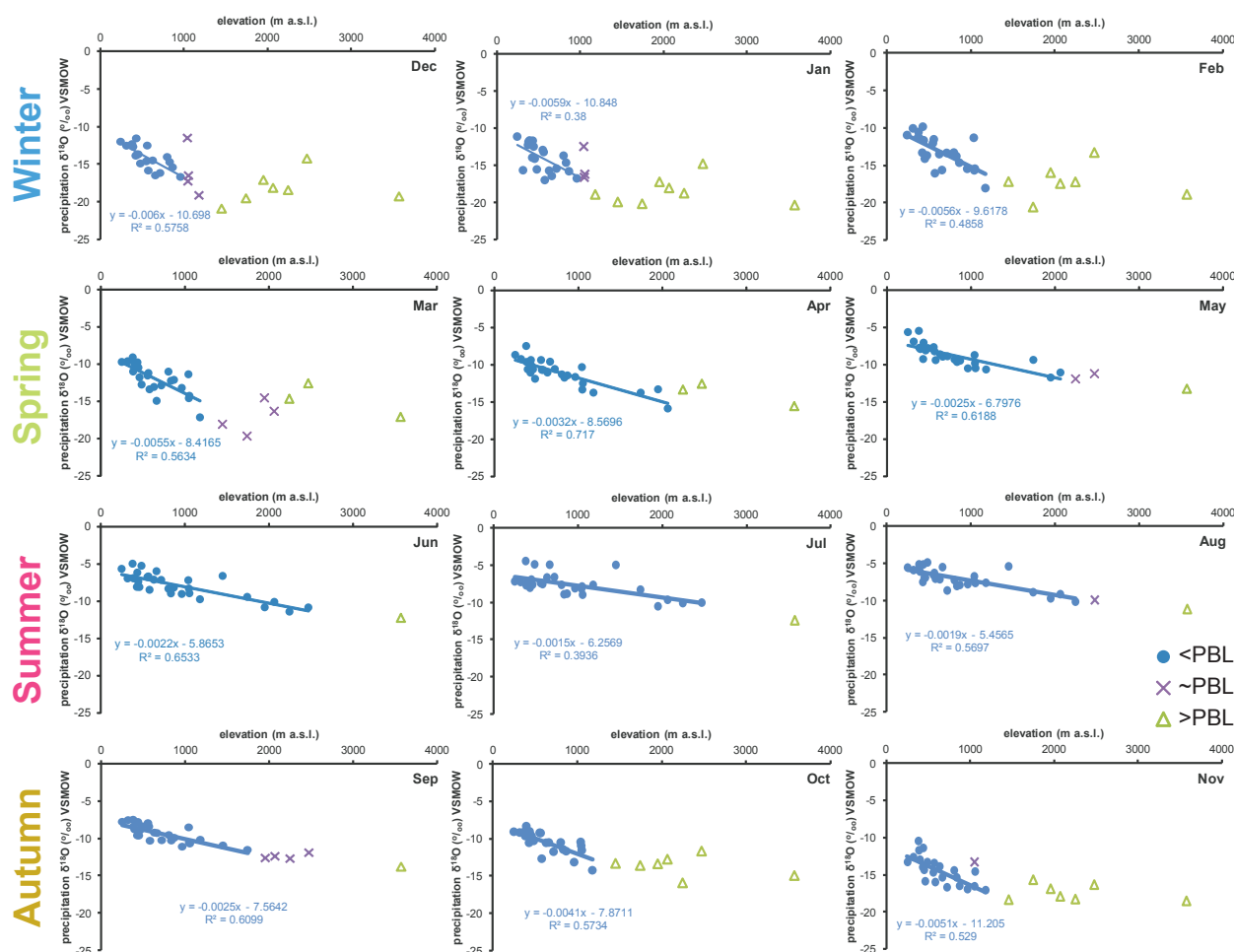


Fig. 2. Monthly amount-weighted stable oxygen isotope composition of precipitation over Switzerland and its border zone. Blue dots represent stations that were always below the planetary boundary layer (PBL), green triangles represent stations that were always above the PBL, while purple crosses represent stations that were occasionally above the PBL during the 1995–2000 period. Regression equations fitted to the stations below the PBL are given for each month.

seasons were estimated by linear interpolation regarding the gradually changing character of this parameter (e.g. Kirchner et al., 2013). Finally, -5 K km^{-1} was used for the moist adiabatic lapse rate.

The calculation gave a numerical hint that atmospheric stratification is likely to be characterized by seasonal contrast (Table 1). It is shown that conditionally unstable atmosphere situations indicate a higher tendency to convective processes occurring in summer, as expected from the seasonal pattern of meteorological parameter for the Alps, while positive values of N_m suggest stratified atmosphere conditions for the Alpine winter. As general winter (summer) season atmospheric conditions in the Alpine atmosphere are less (more) favourable for convective processes, static atmospheric stability and stratification is more pronounced in winter when moistened air is dominant in shallow cyclonic systems. Therefore, the dichotomous winter pattern could be explained by the characteristically shal-

lower vertical atmospheric mixing height during winter season. The Alpine isotopic profile provides empirical support for Galewsky's (2009) simulations of stratified atmospheric flow on orographic precipitation isotopic ratios lacking vertical depletion. The precipitation over the higher terrain is dominantly associated with the large-scale baroclinic systems, while orography induced mesoscale dynamical effects (turbulence, flow deflection) forced additional fractionations near the surface, most probably in the shear layer sitting at the boundary between the blocked lower flow and the unblocked baroclinic flow. This can help to explain the “anomalous” deflected altitudinal isotopic profiles reported by many studies.

A recent study at a prominent high relief, southern Tibet, found that precipitation $\delta^{18}\text{O}$ does not only reflect local climatic conditions but also integrates regional upstream convective activity and precipitation (Gao et al., 2013).

Table 1. Monthly estimates of squared moist Brunt–Väisälä frequency (N_m^2) for southern and northern side of the European Alps. Unreal cases ($N_m^2 < 0$) indicate unstable atmosphere, while positive values indicate static stability.

	Jan	Feb	Mar	Apr	May	Jun	Jul	Aug	Sep	Oct	Nov	Dec
N	0.0066	0.0065	0.0052	0.0035	$N_m^2 < 0$	$N_m^2 < 0$	$N_m^2 < 0$	$N_m^2 < 0$	$N_m^2 < 0$	0.0035	0.0052	0.0066
S	0.0038	0.0037	$N_m^2 < 0$	$N_m^2 < 0$	$N_m^2 < 0$	$N_m^2 < 0$	$N_m^2 < 0$	$N_m^2 < 0$	$N_m^2 < 0$	$N_m^2 < 0$	$N_m^2 < 0$	0.0038

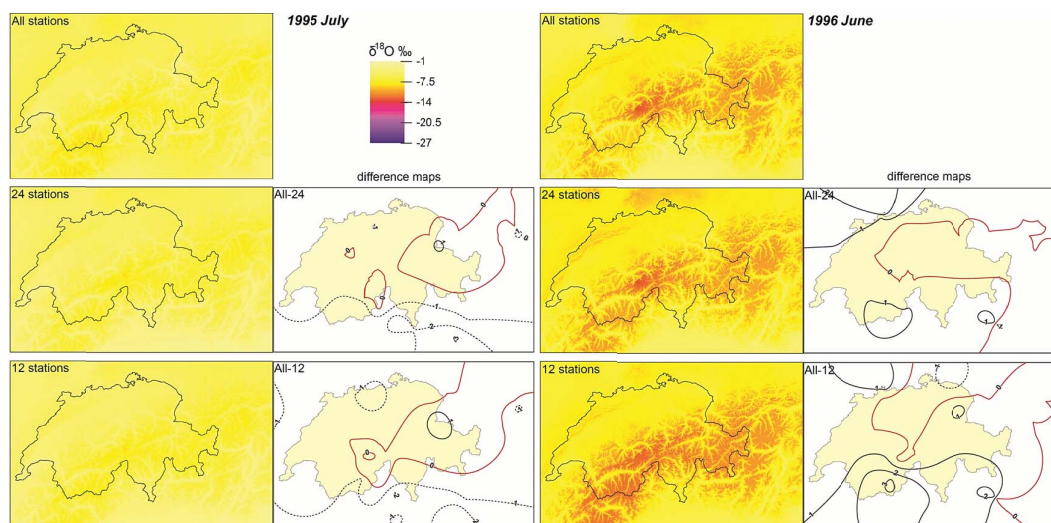


Fig. 3. Precipitation oxygen isoscapes for Switzerland derived for July 1995 and June 1996. Top map shows the isoscape obtained using all available stations. The longest-running 24 and 12 station records have been used for the middle and bottom maps, respectively. The difference map, obtained after grid computed with reduced data set was subtracted from the full one, is shown to the right of the corresponding subset-derived map. Isolines for positive values are shown by the bold lines, while negative values are shown by the dashed lines. The zero isoline is red.

A “classical” atmospheric parameter quantifying the penetration depth to which surface processes influence the atmosphere conditions is the planetary boundary layer heights (Hanna, 1969). Therefore we used a recently developed monthly resolved gridded PBL data set (von Engel and Teixeira, 2013) to facilitate the incorporation of the seasonally changing stratification feature in the Alpine region to the isoscape model (see Sect. 2.3.).

3.3 Monthly $\delta^{18}\text{O}_p$ isoscapes for 1995–1996 and experience with data set reduction tests

The full set of maps (72 isoscapes and 48 difference maps) and the derived data set can be found in the Supplement (Figs. S5, 6). Following a careful evaluation of the spatial patterns, as a compromise, we have selected only six monthly sets of maps to illustrate the major findings.

The twelve longest-running station records, unfortunately, are usually not enough to reproduce the maps derived from the full data set, except for a few summer months like July 1995 or June 1996 (Fig. 3). As noted above, atmospheric stability is the lowest in this season, corresponding to deepest

vertical mixing and highest frequencies of convective processes.

A critical region where regional pattern frequently occurred is the Valais. These more depleted (e.g. May 1996) or enriched (e.g. July 1996) patterns cannot be reproduced with the 12 longest-running station records, but are relatively well captured when at least one station is included, such as Visp, in the 24 group (Fig. 4).

Another critical region is the eastern sector of Switzerland. Maps calculated from the reduced data set often fail to capture the correct values in this region (Fig. 5). It is clear from the difference maps that this is not a station error because the anomaly field usually shows a dipole structure with the stations Pontresina and Vaduz at the poles. The error can be as large as 2 to 4 ‰. It was surprising that in certain months the map calculated from 24 stations showed larger differences over this sector than the map based on 12 stations. It is suspected that this strange situation is due to Säntis, which is included in the 24-station group.

According to our test calculations, with reduced station subsets it will be possible to extend this biannual data set back (i) to 1992 with maintained fidelity only limited by the earliest monitoring data from the Graubünden-Liechtenstein

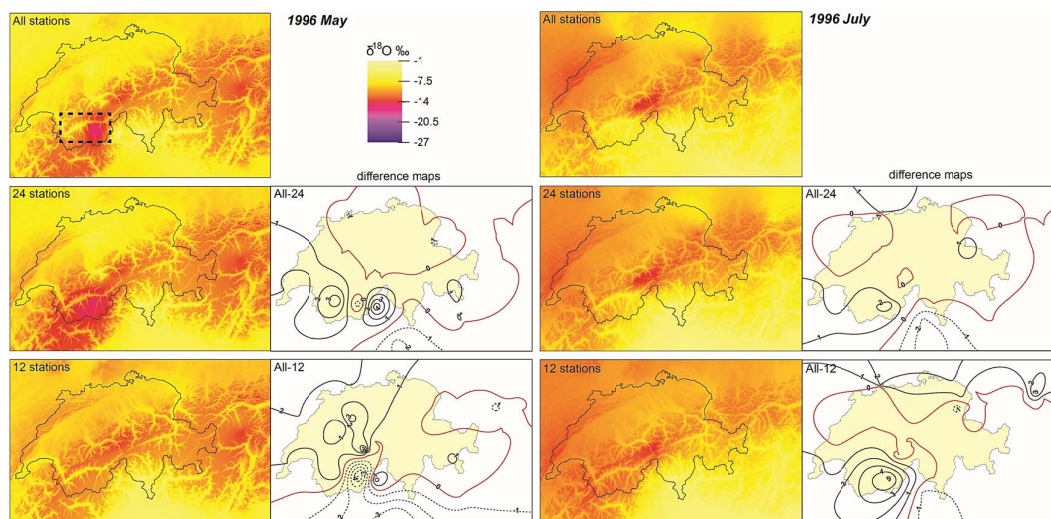


Fig. 4. Precipitation oxygen isoscapes for Switzerland derived for May 1996 and July 1996. Dashed rectangle frames Valais. For further explanation see the caption of Fig. 3.

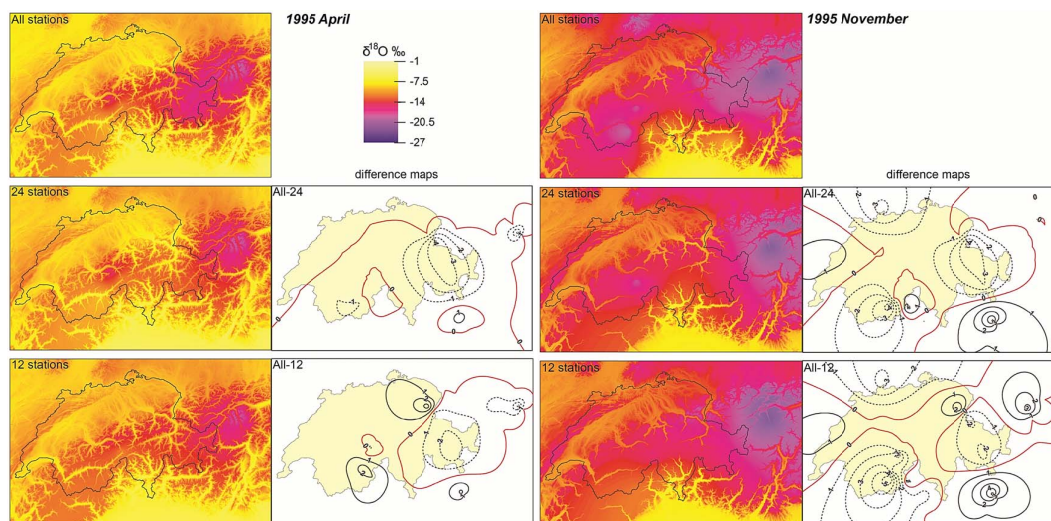


Fig. 5. Precipitation oxygen isoscapes for Switzerland derived for April 1995 and November 1995. For further explanation see the caption of Fig. 3.

region, namely July 1992 (Vaduz), and (ii) to even a decade before but at the expense of faded reliability over the eastern sector, especially east from the Upper Rhine Valley.

Finally, we remark that mountain stations from the northern Italian network (Graniga and Presolana) frequently define some local anomaly pattern. This occurs in any season so we are quite confident that it is not an artefact due to PBL sorting of the stations. These mountain stations tend to diverge from their nearby low elevation neighbour while the lowland station agrees well with the next nearest one. This suggests that Graniga and Presolana might own locally restricted isotopic patterns at those months. In the presented interpolation approach it is unfeasible to reduce the radius of

influence only for these two stations; therefore, we have to face the risk that their anomalies are probably extended over a larger domain. However, as documented by the difference maps (e.g. Fig. 5), the anomaly fields fade out generally before the Swiss border and hence the peculiar behaviour of those two stations does not exert a significant bias in the interpolation over the Swiss territory.

3.4 Further implications

The presented results might have significant implications for other related fields using stable precipitation isotopes. The lack of altitude dependence during wintertime passed on its influence also to the multiannual mean $\delta^{18}\text{O}_p$ values of

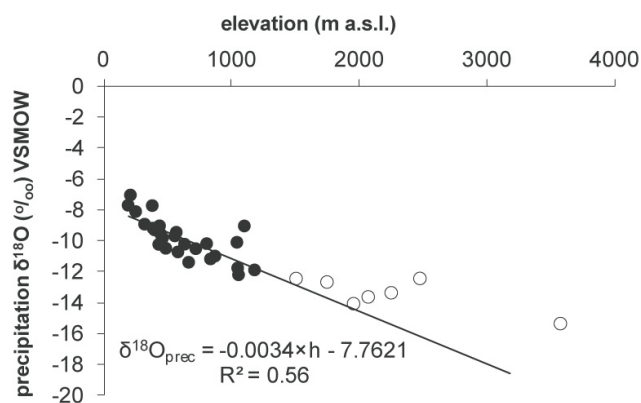


Fig. 6. Multiannual (1995–2000) amount-weighted mean stable oxygen isotope ratios from the Alpine region as a function of stations' elevation. Regression is fitted to the subset of stations below 1200 m a.s.l. (filled circles).

the high elevation stations (Fig. 6). Projected values (black line) based on the station records below 1200 m a.s.l. are doubtlessly more negative above ~ 2000 m a.s.l. than the measured values. This fact might introduce an additional uncertainty to the methodological background of palaeoaltimetry (Blisniuk and Stern, 2005; Rowley and Garzzone, 2007). First, when the uplifted terrain penetrated the regional PBL, or as an equivalent situation reached a critical height when the “usual” atmospheric flow was prone to stratification, the precipitation stable isotope values most probably deviated from the normal altitude dependence, leading to a dampened estimate, i.e. altitudes would be underestimated. On the contrary, if the PBL height was increased (static stability decreased) due to better mixing (warming, enhanced pressure gradient), the correspondent $\delta^{18}\text{O}_p$ change would be misinterpreted as an uplift without any real orogenic activity. This concern tends to strengthen the criticism of the methodological grounds of palaeoaltimetry (Ehlers and Poulsen, 2009; Galewsky, 2009).

Until recently the long-term stable isotope records from Alpine ice cores were regarded to consist mainly of summer precipitation and thus reflect long-term trends in local high-elevation summer air temperature (Schöner et al., 2002). One of the key arguments for the above statement was the lack of the expected very depleted winter snow layer in the Alpine firn/ice core profiles. Present results suggest that one should not expect further decrease in winter $\delta^{18}\text{O}_p$ values above a certain level, roughly above the mean winter PBL. It could be an interesting future exercise to compare the $\delta^{18}\text{O}$ records from the Alpine ice cores (e.g. Mariani et al., 2012) to our estimated high resolution site-specific isotope signal.

4 Conclusions

Scrutiny of amount-weighted mean monthly $\delta^{18}\text{O}_p$ of a large set of Alpine stations provided new insights into the seasonal changes of $\delta^{18}\text{O}_p$ over high reliefs. In addition, a computation scheme has been designed to derive monthly maps/grids of $\delta^{18}\text{O}_p$ using PBL and topographic data. The method was then tested for the studied Alpine region.

The 12 longest-running station records were usually insufficient to map the regional $\delta^{18}\text{O}$ patterns. Valais and the eastern sector of Switzerland often have unique $\delta^{18}\text{O}$ signatures, which can be captured only when at least one station from these regions is used.

The presented data set allowing point estimation of $\delta^{18}\text{O}_p$ with monthly resolution, and more particularly the extended record to be developed using the present approach, will most likely be valuable input or auxiliary data for the Alpine hydrological modelling efforts, providing a basis for regional ecological modelling (e.g. migratory studies) and the crucial local isotopic target throughout practically the entire western Alpine region for calibration of palaeoclimate proxy records (e.g. from tree rings, ice cores or speleothems) and could be employed as a reference data set for regional isotope-enabled circulation models. The most exciting exercise could be the comparison to Alpine ice core $\delta^{18}\text{O}$ signals as these records are regarded as (i) the most direct archives of past precipitation and (ii) being independent of the source data used for the calibration of the presented geostatistical interpolation. The combination of the $\delta^{18}\text{O}_p$ grids with Lagrangian moisture source diagnostics (Sodemann and Zubler, 2010), for instance, offer an advanced interpretation of Alpine sub-regional moisture regime and its implications for water stable isotope compositions.

The general winter season atmospheric conditions in the Alpine atmosphere are less favourable for convective processes (colder air temperature, lower environmental lapse rate, and lower specific humidity). Cold conditions favour atmosphere stability, which inhibits vertical air motions. Therefore, the observed winter Alpine isotopic profile supports simulated effects (Galewsky, 2009) of stratified atmospheric flow on orographic precipitation isotopic ratios.

Decoupled regimes below and above the PBL height received little attention in spatial precipitation isotope modelling efforts. Present results point out that PBL location is recommended to be taken into account for future models developed for stable isotope composition runs of precipitation over high reliefs.

Supplementary material related to this article is available online at <http://www.atmos-chem-phys.net/14/1897/2014/acp-14-1897-2014-supplement.zip>.

Acknowledgements. Special thanks to H. Bürki, U. Schotterer, R. Kozel and M. Schürch for their help with the Swiss precipitation samples, to A. Longinelli and E. Selmo for the data from Italy and to the researchers who contributed data to the Global Network of Isotopes in Precipitation and the Austrian Network of Isotopes in Precipitation. A. von Engel is acknowledged for the PBL data. ISO-TREE (Sciex code:10.255.) and iTREE (CRSII3 13695) supported the research. We gratefully acknowledge financial support by the Swiss Federal Office for the Environment (FOEN). Z. Kern expresses thanks to the Lendület program of the Hungarian Academy of Sciences (LP2012-27/2012).

Edited by: M. Heimann

References

- Ambach, W., Dansgaard, W., Eisner, H., and Møller, J.: The altitude effect on the isotopic composition of precipitation and glacier ice in the Alps, *Tellus B*, 20, 595–600, 1968.
- Baker, D., Moser, H., Oerter, H., Stichler, W. and Reinwarth, O.: Comparison of the ^2H and ^{18}O content of ice cores from a temperate Alpine glacier (Vernagtferner, Austria) with climatic data, *Zeitschrift für Gletscherkunde und Glazialgeologie*, 21, 389–395, 1985.
- Blisniuk, P. M. and Stern, L. A.: Stable isotope paleoaltimetry: A critical review, *Am. J. Sci.*, 305, 1033–1074, 2005.
- Bowen, G. J.: Isoscapes: Spatial pattern in isotopic biogeochemistry, *Annu. Rev. Earth Pl. Sc.*, 38, 161–187, 2010a.
- Bowen, G. J.: Statistical and geostatistical mapping of precipitation water isotope ratios, in: *Isoscapes: Understanding Movement, Pattern, and Process on Earth through Isotope Mapping*, edited by: West, J. B., Bowen, G. J., Dawson, T. E., and Tu, K. P., New York, Springer, 139–160, 2010b.
- Bowen, G. J. and Revenaugh, J.: Interpolating the isotopic composition of modern meteoric precipitation, *Water Resour. Res.* 39, 1299, doi:10.1029/2003WR002086, 2003.
- Bowen, G. J. and Wilkinson, B.: Spatial distribution of $\delta^{18}\text{O}$ in meteoric precipitation, *Geology*, 30, 315–318, 2002.
- Chimani, B., Matulla, C., Böhm, R., and Hofstätter, M.: A new high resolution absolute temperature grid for the Greater Alpine Region back to 1780, *Int. J. Climatol.*, 33, 2129–2141, doi:10.1002/joc.3574, 2013.
- Cressie, N.: *Statistics for spatial data*, New York, Wiley, 1993.
- Durrant, D. R. and Klemp, J. B.: On the effects of moisture on the Brunt–Väisälä frequency, *J. Atmos. Sci.*, 39, 2152–2158, 1982.
- Ehlers, T. A. and Poulsen, C. J.: Influence of Andean uplift on climate and paleoaltimetry estimates, *Earth Planet. Sc. Lett.*, 281, 238–248, 2009.
- Farr, T. G., Rosen, P. A., Caro, E., Crippen, R., Duren, R., Hensley, S., Kozubick, M., Paller, M., Rodriguez, E., Roth, L., Seal, D., Shaffer, S., Shimada, J., Umland, J., Werner, M., Oskin, M., Burbank, D., and Alsdorf, D.: The Shuttle radar topography mission, *Rev. Geophys.*, 45, RG2004, doi:10.1029/2005RG000183, 2007.
- Frei, C. and Schär, C.: A precipitation climatology of the Alps from high-resolution rain-gauge observations, *Int. J. Climatol.*, 18, 873–900, doi: 10.1002/(SICI)1097-0088(19980630)18:8<873::AID-JOC255>3.0.CO;2-9, 1998.
- Fröhlich, K., Kralik, M., Papesch, W., Rank, D., Scheifinger, H., and Stichler, W.: Deuterium excess in precipitation of Alpine Regions – Evaluation of sub-cloud evaporation and moisture recycling, *Isotopes Environ. Health Stud.*, 44, 61–70, 2008.
- Gao, J., Masson-Delmotte, V., Risi, C., He, Y., and Yao, T.: What controls precipitation $\delta^{18}\text{O}$ in the southern Tibetan Plateau at seasonal and intra-seasonal scales? A case study at Lhasa and Nyalam, *Tellus B*, 65, 21043, doi:10.3402/tellusb.v65i0.21043, 2013.
- Galewsky, J.: Orographic precipitation isotopic ratios in stratified atmospheric flows: Implications for paleoelevation studies, *Geology*, 37, 791–794, doi:10.1130/G30008A.1, 2009.
- Hanna, S. R.: The thickness of the planetary boundary layer, *Atmos. Environ.*, 3, 519–536, 1969.
- Haylock, M. R., Hofstra, N., Klein Tank, A. M. G., Klok, E. J., Jones, P. D., and New, M.: A European daily high resolution gridded data set of surface temperature and precipitation for 1950–2006, *J. Geophys. Res.*, 113, D20119, doi:10.1029/2008jd010201, 2008.
- Henne, S., Furger, M., Nyeki, S., Steinbacher, M., Neining, B., de Wekker, S. F. J., Dommien, J., Spichtinger, N., Stohl, A., and Prévôt, A. S. H.: Quantification of topographic venting of boundary layer air to the free troposphere, *Atmos. Chem. Phys.*, 4, 497–509, doi:10.5194/acp-4-497-2004, 2004.
- Holdsworth, G., Fogarasi, S., and Krouse, H. R.: Variation of the stable isotopes of water with altitude in the Saint Elias Mountains of Canada, *J. Geophys. Res.*, 96, 7483–7494, doi:10.1029/91JD00048, 1991.
- Holko, L., Dosa, M., Michalko, J., Kostka, Z., and Sanda, M.: Isotopes of Oxygen-18 and Deuterium in precipitation in Slovakia, *J. Hydrol. Hydromech.*, 60, 265–276, 2012.
- Hunjak, T., Lutz, H. O., and Roller-Lutz, Z.: Stable isotope composition of the meteoric precipitation in Croatia, *Isotopes Environ. Health Stud.*, 49, 336–345, doi:10.1080/10256016.2013.816697, 2013.
- IAEA: Global Network of Isotopes in Precipitation, The GNIP Database 2010, available at: <http://www.isohis.iaea.org> (last access: 9 July 2012), 2010.
- Kralik, M., Papesch, W., and Stichler, W.: Austrian Network of Isotopes in Precipitation (ANIP): Quality assurance and climatological phenomenon in one of the oldest and densest networks in the world, *Isot. Hydrol. Integr. Water Resour. Manag.*, 23, 146–149, 2003.
- Liebminger, A., Haberhauer, G., Varmuza, K. G., Papesch, W., and Heiss, G.: Modeling the Oxygen 18 concentration in precipitation with ambient climatic and geographic parameters, *Geophys. Res. Lett.*, 33, L05808, doi:10.1029/2005GL025049, 2006.
- Liebminger, A., Haberhauer, G., Papesch, W., and Heiss, G.: Footprints of climate in groundwater and precipitation, *Hydrol. Earth Syst. Sci.*, 11, 785–791, doi:10.5194/hess-11-785-2007, 2007.
- Liotta, M., Grassa, F., D’Alessandro, W., Favara, R., Gagliano Candela, E., Pisciotta, A., and Scaletta, C.: Isotopic composition of precipitation and groundwater in Sicily, Italy, *Appl. Geochem.*, 34, 199–206, doi:10.1016/j.apgeochem.2013.03.012, 2013.
- Longinelli, A. and Selmo, E.: Isotopic composition of precipitation in Italy: a first overall map, *J. Hydrol.*, 270, 75–88, 2003.
- Longinelli, A. and Selmo, E.: Isotopic composition of precipitation in Northern Italy: Reverse effects of anomalous climatic events, *J. Hydrol.*, 329, 471–476, 2006.
- Lykoudis, S. P. and Argiriou, A. A.: Gridded data set of the stable isotopic composition of precipitation over the eastern

- and central Mediterranean, *J. Geophys. Res.*, 112, D18107, doi:10.1029/2007JD008472, 2007.
- Lykoudis, S. P., Argiriou, A. A., and Dotsika, E.: Spatially interpolated time series of $\delta^{18}\text{O}$ in Eastern Mediterranean precipitation, *Global Planet. Change*, 71, 150–159, 2010.
- Mariani, I., Eichler, A., Brönnimann, S., Auchmann, R., Jenk, T. M., Leuenberger, M. C., and Schwikowski, M.: Temperature and precipitation signal in two Alpine ice cores over the period 1961–2001, *Clim. Past Discuss.*, 8, 5867–5891, doi:10.5194/cpd-8-5867-2012, 2012.
- Meehan, T. D., Giermakowski, J. T., and Cyran, P. M.: GIS-based model of stable hydrogen isotope ratios in North American growing-season precipitation for use in animal movement studies, *Isotopes Environ. Health Stud.*, 40, 291–300, 2004.
- Moser, H. and Stichler, W.: Deuterium and oxygen-18 contents as an index of the properties of snow cover, *Symposium on Snow Mechanics*, IAHS Publ. 114, 122–135, 1974.
- Nyeki, S., Kalberer, M., Colbeck, I., De Wekker, S., Furger, M., Gaggeler, H. W., Kossmann, M., Lugauer, M., Steyn, D., Weingartner, E., Wirth, M., and Baltensperger, U.: Convective boundary layer evolution to 4 km asl over high-alpine terrain: airborne lidar observations in the Alps, *Geophys. Res. Lett.*, 27, 689–692, 2000.
- Rotunno, R. and Houze, R. A.: Lessons on orographic precipitation from the Mesoscale Alpine Programme, *Q. J. Roy. Meteor. Soc.*, 133, 811–830, doi:10.1002/qj.67, 2007.
- Rowley, D. B. and Garzione, C. N.: Stable isotope-based paleolatimetry, *Annu. Rev. Earth Pl. Sc.*, 35, 463–508, 2007.
- Scherrer, S. C., Croci-Maspoli, M., van Geijtenbeek, D., Hotz, C., Frei, C., and Appenzeller, C.: Operational quality control of daily precipitation using spatio-climatological plausibility testing, *Meteorol. Z.*, 20, 397–407, doi:10.1127/0941-2948/2011/0236, 2011.
- Schwikowski, M. and Eichler, A.: Alpine Glaciers as Archives of Atmospheric Deposition, in: *Alpine Waters*, edited by: Bundi, U., 141–150, Springer-Verlag Berlin, Heidelberg Platz 3, 14197 Berlin, Germany, doi:10.1007/978-3-540-88275-6_7, 2010.
- Schotterer, U., Fröchlich, K., Gaggeler, H. W., Sandjorj, S., and Stichler, W.: Isotope records from Mongolian and Alpine ice cores as climate indicators, *Clim. Change*, 36, 518–530, 1997.
- Schotterer, U., Stocker, T., Bürki, H., Hunziker, J., Kozel, R., Grasso, D. A., and Tripet, J.-P.: Das Schweizer Isotopen-Messnetz. Trends 1992–1999, *Gas-Wasser-Abwasser*, 10, 733–741, 2000.
- Schotterer, U., Schürch, M., Rickli, R., and Stichler, W.: Wasserisotopen in der Schweiz, *Gas-Wasser-Abwasser*, 12, 1073–1081, 2010.
- Schöner, W., Auer, I., Böhm, R., Keck, L., and Wagenbach, D.: Spatial representativity of air-temperature information from instrumental and ice-core-based isotope records in the European Alps, *Ann. Glaciol.*, 35, 157–161, 2002.
- Schürch, M., Kozel, R., Schotterer, U., and Tripet, J. P.: Observation of isotopes in the water cycle – the Swiss National Network (NISOT), *Environ. Geol.*, 45, 1–11, 2003.
- Seidel, D. J., Zhang, Y., Beljaars, A., Golaz, J. C., Jacobson, A. R., and Medeiros, B.: Climatology of the planetary boundary layer over the continental United States and Europe, *J. Geophys. Res.*, 117, D17106, doi:10.1029/2012JD018143, 2012.
- Siegenthaler, U. and Oeschger, H.: Correlation of ^{18}O in precipitation with temperature and altitude, *Nature*, 285, 314–317, 1980.
- Sodemann, H. and Zubler, E.: Seasonal and inter-annual variability of the moisture sources for Alpine precipitation during 1995–2002, *Int. J. Climatol.*, 30, 947–961, 2010.
- Terzer, S., Wassenaar, L. I., Araguás-Araguás, L. J., and Aggarwal, P. K.: Global isoscapes for $\delta^{18}\text{O}$ and $\delta^2\text{H}$ in precipitation: improved prediction using regionalized climatic regression models, *Hydrol. Earth Syst. Sci.*, 17, 4713–4728, doi:10.5194/hess-17-4713-2013, 2013.
- Thompson, L. G., Mosley-Thompson, E., Davis, M. E., Lin, P. N., Henderson, K. A., Cole-Dai, J., Bolzan, J. F., and Liu, K. B.: Late Glacial Stage and Holocene tropical ice core records from Huascarán, Peru, *Science*, 269, 46–50, 1995.
- Vachon, R. W., Welker, J. M., White, J. W. C., and Vaughn, B. H.: Monthly precipitation isoscapes ($\delta^{18}\text{O}$) of the United States: Connections with surface temperatures, moisture source conditions, and air mass trajectories, *J. Geophys. Res.*, 115, D21126, doi:10.1029/2010jd014105, 2010.
- von Engel, A. and Teixeira, J.: A planetary boundary layer height climatology derived from ECMWF re-analysis data, *J. Climate*, 26, 6575–6590, doi:10.1175/JCLI-D-12-00385.1, 2013.
- Welker, J. M.: ENSO effects on $\delta^{18}\text{O}$, $\delta^2\text{H}$ and d-excess values in precipitation across the U.S. using a high-density, long-term network (USNIP), *Rapid Commun. Mass Sp.*, 26, 1893–1898, 2012.
- West, J. B., Bowen, G. J., Dawson, T. E., and Tu, K. P. (Eds): *Isoscapes Understanding movement, pattern, and process on Earth through isotope mapping*, New York, Springer, 2010.